POLITECNICO DI TORINO

UNIVERSITÀ DEGLI STUDI DI TORINO

Human Liver Stem Cells and Derived Products in Experimental Models of Liver Ischemia Reperfusion Injury and of Liver Isolated Normothermic Perfusion

PhD Program in Bioengineering and Medical-Surgical Sciences

XXX Cycle

Candidate: Dott.ssa Giorgia Catalano

Tutor: Prof. Mauro Salizzoni

Academic Year
2016-2017

TABLE OF CONTENTS

1. INTRODUCTION

Ischemia reperfusion injury (IRI) is an Antigen (Ag)-independent inflammatory event that affects several clinical settings, including surgical procedures such as liver resection and liver transplantation. IRI is still a major concern in the transplantation setting, causing up to 10% of early graft failure and leading to a higher incidence of acute and chronic rejection[1]. IRI is initiated by Kuppfer cells and hepatocytes through a massive production of reactive oxygen species (ROS) during the ischemic phase and, in a major degree, during the post-reperfusion phase. ROS directly damage hepatocytes and endothelial cells and promote the recruiment of neutrophils and T-cells, starting an inflammatory cascade that triggers apoptosis and necrosis. Clearly, there is a widespread interest regarding possible means to reduce the possibility of this event.

Human liver stem cells (HLSC) are human hepatocyte progenitors cells expressing both markers of stem cells and hepatocytes. HLSC have been isolated in 2006 at the University of Turin by culturing human hepatocytes in stringent culture conditions. Adult human liver stem-like cells (HLSC) may be useful in regenerative medicine because they are easily expandable and have multiple differentiating capabilities[2,3]. They express several mesenchymal (CD29, CD73, CD44, CD90) and embryonic markers (Nanog, Sox2, Musashi1, Oct 3/4, Pax2), but not haematopoietic ones. Moreover, HLSC express albumin, alpha-fetoprotein and cytokeratin 18, supporting their partial hepatic commitment[2]. We showed that HLSC could restore hepatic function and improve survival in a model of fulminant liver failure in immunodeficient mice[3] and could generate hepatic-like tissue when seeded in liver acellular scaffolds[4].

Stem cell-derived extracellular vesicles (EV) are a heterogeneous population of cell-secreted vesicles which play a pivotal role in cell-to-cell communication; they carry specific subsets of

mRNA and miRNA that regulate target cells behaviour[5,6]. Many *in vitro* and *in vivo* studies demonstrated the EV therapeutic potential, showing that their beneficial effect is comparable to that of the stem cells they derive from[7,8,9,10,11].

2. ISOLATION, CHARACTERIZATION AND CULTURE OF HLSC

HLSC were isolated from human cryopreserved hepatocytes obtained from Lonza Bioscience (Basel, Switzerland) and characterized[2,3]. HLSC were cultured in a medium containing a 3:1 proportion of α-minimum essential medium and endothelial cell basal medium-1, supplemented with L-glutamine 2 mM, penicillin 100 U/mL, streptomycin 100 μg/mL and 10% foetal calf serum (α-MEM/EBM/FCS), and maintained in a humidified 5% CO_2 incubator at 37°C. HLSC at passages 5 to 8 and 80% confluence were used in all experiments.

3. ISOLATION OF DIL-LABELLED HLSC-EV

The HLSC were previously labelled with the DIL Stain (1,1'-Dioctadecyl-3,3,3',3'-Tetramethylindocarbocyanine Perchlorate 'DiI'; DiIC18(3)) (Molecular Probes Life Technology, New York, NY, USA)[11] and cultured. Once at 80% confluence, cells were starved overnight in RPMI/P-S medium deprived of FCS at 37°C in a humidified incubator with 5% CO_2. Supernatants were collected, centrifuged at 3,500 rpm for 15 minutes to remove cell debris, and submitted to ultracentrifugation at 100,000 g for 2 hours at 4°C (Beckman Coulter Optima L-90 K, Fullerton, CA, USA). EV were collected and used fresh or stored at −80°C after re-suspension in RPMI plus 1% dimethyl sulfoxide. No difference in

biological activity was observed between fresh and stored EV (data not shown). Quantification and size distribution of EV were performed using NanoSight LM10 (NanoSight Ltd, Minton Park, UK)[9].

4. FIRST PROJECT

"Extracellular vesicles from human liver stem cells reduce injury in an ex vivo normothermic hypoxic rat liver perfusion model"

Liver transplantation (LT) is currently the only successful therapy for end-stage liver disease. Yet, the discrepancy between organs and candidates remains its strongest limit. Several new strategies are under investigation for their potential to ameliorate the transplant process and expand the donor pool[12].

Static cold storage (SCS) is the gold standard for organ preservation. The rapid cooling of the liver by icy fluids together with the protective effect of specific solutions, slows hepatocellular metabolism and reduces ATP depletion and loss of cellular integrity[13]. Unfortunately, SCS is imperfect in preserving organs from extended criteria donors[14].

Normothermic Machine Perfusion (NMP) is an innovative alternative to SCS. Through an extracorporeal perfusion circuit, it keeps the organ at physiological temperature while providing oxygen and nutrients continuously[15]. At variance with SCS, NMP allows real-time monitoring of biomarkers and hemodynamic parameters that correlate with organ viability, making the transplant process more objective. Animal studies demonstrated the superiority of NMP compared to SCS[16,17,18,19,20,21] and a Phase I study established safety and feasibility of this technique in humans[22]. Furthermore, NMP gives the unique opportunity to treat the liver with pharmacological interventions in the pre-transplant phase[23].

In this study, we set up a short-duration model of *ex vivo* isolated rat liver NMP in which oxygen delivery was kept suboptimal through a low haemoglobin content in the perfusate. In this model, we investigated whether adding HLSC-derived EV (HLSC-EV) to the circuit could result in:

i) their rapid uptake by the liver,

ii) an appreciable reduction of the hypoxic tissue injury.

4.1 Animals

Animal studies were approved by the Ethic Committee of Istituto Superiore di Sanità (N.1164/2015-PR) and conducted in accordance with the National Institute of Health Guide for Care and Use of Laboratory Animals. Male Wistar rats aged 8-12 weeks (200-250 g weight) obtained from Charles Rivers (Italy) were maintained on standard conditions and provided with food and water *ad libitum*.

4.2 Isolation of Rat Livers

Animals were anesthetized through an intramuscular injection of Zolazepam (0.2 mg/Kg) and Xilazyne (16 mg/Kg). After intraperitoneal heparin (1,250 U) administration, a midline laparotomy was performed. The bowel was retracted to expose the liver, with particular attention to portal vein (PV), hepatic artery (HA), inferior vena cava (IVC) and common bile duct (CBD)(Figure 1A-B). The CBD was cannulated with a 22G cannula, the HA was ligated and the PV cannulated with an 18G cannula (Figure 1C-F). After sternotomy, an incision was

made in the right heart ventricle to exsanguinate the animal. The liver was flushed with 40 mL of cold Celsior solution (IGL, France) through the PV (Figure 1G-I). After perfusion, the liver was freed from its ligaments and the suprahepatic IVC, the infrahepatic IVC, the CBD and the PV were transected allowing organ removal. The isolated liver was weighed, placed into a Petri dish filled with ice-cold Celsior solution and transported to the perfusion room.

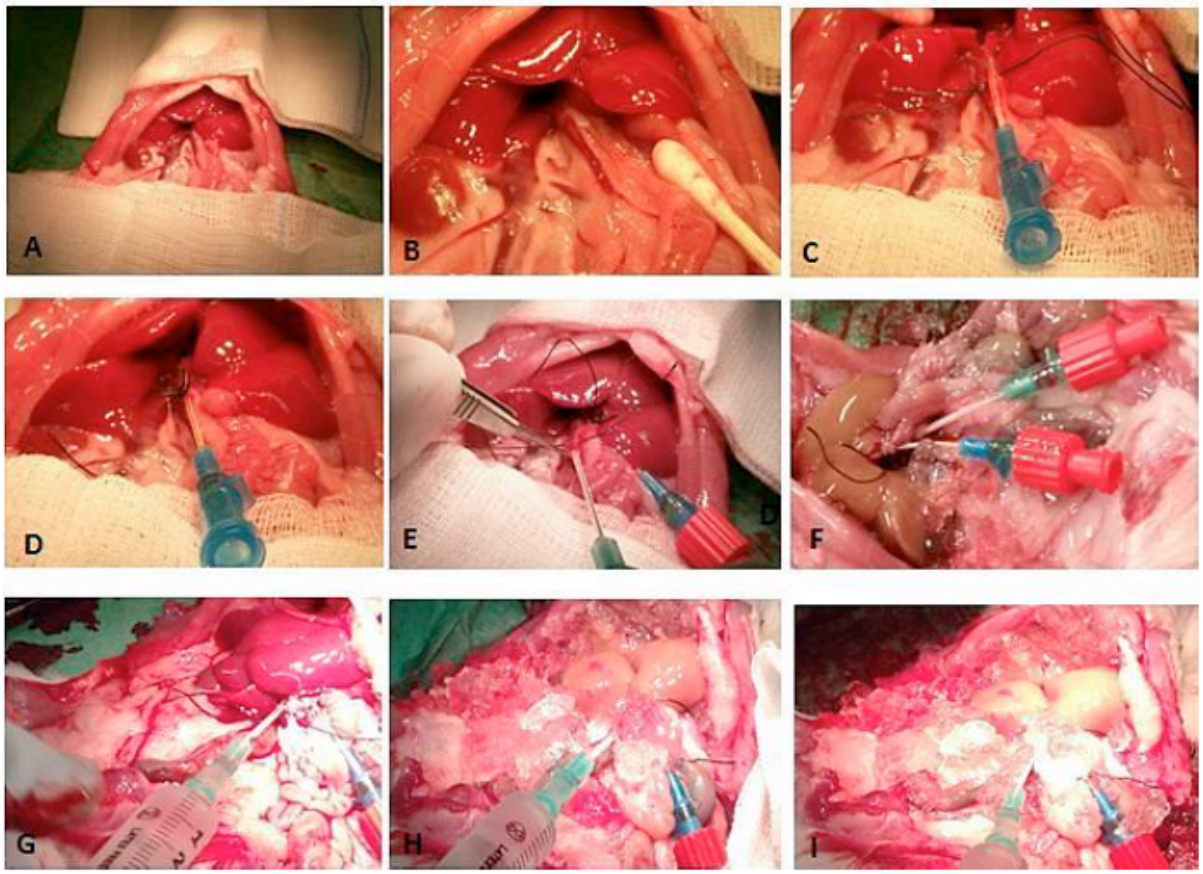

Figure 1. Surgical procedure. **(A)** median laparotomy; **(B)** exposure of the liver pedicle; **(C-D)** cannulation of the CBD; **(E-F)** cannulation of the PV; **(G-H-I)** flushing with cold Celsior solution through the PV.

4.3 Normothermic Machine Perfusion

The NMP circuit was composed of a perfusion chamber (Figure 2A), a peristaltic pump (Figure 2B), an oxygenator (Hollow Fiber Oxygenator D150, Hugo Sachs Elektronik) (Figure 2C) and a bubble trap (Figure 2D). A Transducer Amplifier Module (TAM-D) and a Servo Controller (SCP Type 704) (Harvard Apparatus, Hugo Sachs Elektronik) allowed constant pressure perfusion (8-10 mmHg) and continuous monitoring of perfusate flow (1.1-1.3 mL/min/g liver). The perfusion chamber was linked to a warming circuit made of a thermocirculator (Lauda) with temperature set at 37°C (Figure 2E).

The perfusion solution consisted of phenol red-free Williams E Medium, supplemented with 11.6 mM glucose, 50 U/mL penicillin, 50 μg/mL streptomycin, 5 mM L-glutamine (all from Sigma), 1 U/ml insulin (Lilly, Italy), 1 U/mL heparin (PharmaTex, Italy), named complete Williams Medium. An isovolemic hemodilution was performed by adding 20 mL of fresh rat blood to 50 mL of complete Williams Medium, thus obtaining a mean hematocrit of 9.67 ± 0.66%. This low haemoglobin content (roughly half of what is usually employed in similar perfusion settings)[20] was devised to provide suboptimal oxygen delivery and induce a limited but progressive hypoxic injury[24]. The perfusion solution was gassed with 99% oxygen, and 2 mEq/2 mL of bicarbonate were used to prevent pH fluctuations.

Livers were flushed with complete Williams Medium and connected to the NMP circuit, allowing continuous perfusion at 37°C through the PV cannula for four hours in controlled conditions of flux and pressure. Heparin (500 U) was added hourly during perfusion. A tube was inserted into the CBD cannula to collect bile (Figure 3).

Rat livers undergoing NMP were divided in two groups: NMP alone (NMP group, n=10) and NMP enriched with HLSC-EV (NMP+HLSC-EV group, n=9). In the NMP+HLSC-EV group,

EV were added to the circuit after 15 minutes from perfusion start, in a single dose of $5x10^8$ HLSC-EV/g of liver[10].

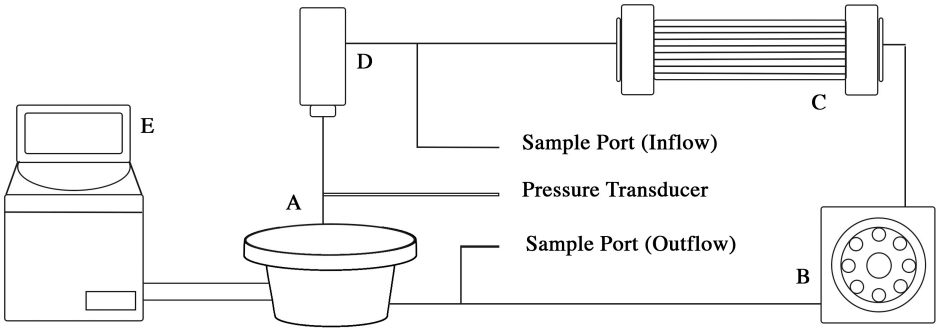

Figure 2. Normothermic Machine Perfusion. A: perfusion chamber; B: peristaltic pump; C: oxygenator; D: bubble trap; E: thermocirculator.

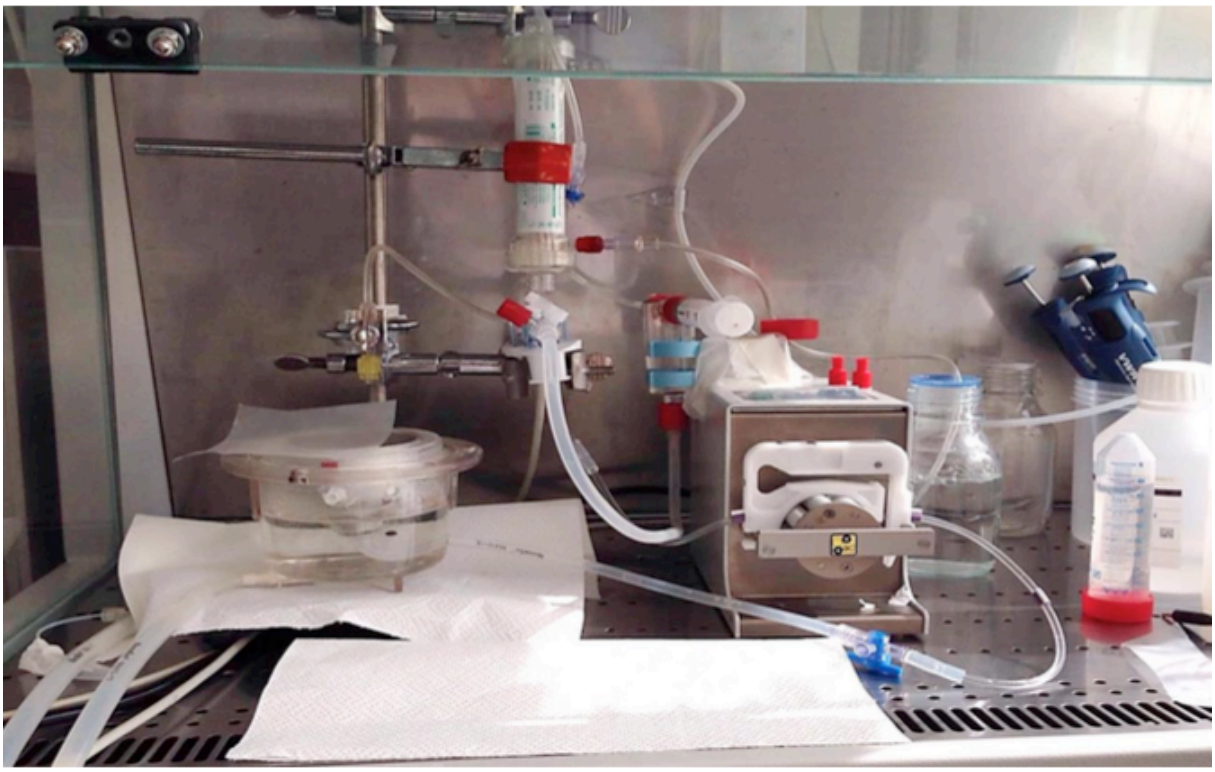

Figure 3. Our Normothermic Machine Perfusion.

4.4 Perfusate Analysis

Blood gas analysis (ABL 705L Radiometer, Copenhagen) was performed hourly during perfusion in inflow and outflow perfusate samples, testing pO_2, pCO_2 and pH. In addition, outflow samples (1 mL) were collected every 60 minutes and centrifuged at 3,500 rpm for 10 minutes at 4°C; the cell-free supernatants were stored at -80°C until aspartate aminotransferase (AST), alanine aminotransferase (ALT) and lactate dehydrogenase (LDH) levels were assessed by the Biochemistry Laboratory, Molinette Hospital, Turin, Italy.

4.5 Immunofluorescence and histological analysis

To analyze the HLSC-EV uptake, two liver lobes were included in Killik OCT medium (Bio-optica) and frozen at -80°C; then serial slides were cut (3-5 μm) by a cryostat and fixed in acetone. After rinsing in phosphate-buffered saline (PBS), the slides were incubated with a blocking solution of 3% bovine serum albumin and 0.1% Tween-20 in PBS for 1 hour at room temperature, and then incubated overnight at 4°C with a primary antibody directed against rat cytochrome P450-4A (Invitrogen) at the dilution of 1:50. After washing in PBS, the slides were incubated with the secondary antibody Alexa Fluor 488 (Invitrogen) for 1 hour at room temperature. Finally, nuclei were stained with 4',6-diamidino-2-phenylindole and slides were mounted with Fluoromount (Sigma). Microscopy analysis was performed using a Cell Observer SD-ApoTome laser scanning system (Carl Zeiss).

Two other liver lobes were formalin fixed and paraffin embedded, then sections were performed in the areas where the macroscopic aspect was most altered. Hematoxylin-eosin staining was used. The severity of histological damage was blindly scored by an experienced

pathologist following modified Suzuki criteria[25]. According to this classification, sinusoidal congestion, hepatocyte necrosis and ballooning degeneration are graded from 0 to 4. Each liver final score was determined by the summation of the grades for the three items. Immunohistochemistry by terminal deoxynucleotidyl transferase dUTP nick-end labelling (TUNEL) was performed to detect apoptosis[26]. Positive and negative TUNEL cells were blindly counted on 20 microscopic fields at 200× magnification, then the apoptosis index was calculated as the ratio between the number of positive cells and of total cells.

4.6 Real-Time Quantitative RT-PCR

RNA was extracted from all paraffin embedded liver samples using RecoverAll™ Total Nucleic Acid Isolation Kit for FFPE (Invitrogen), then quantified spectrophotometrically (NanoDrop 2000^{TM}, Thermo Scientific). The subsequent analyses could be performed on more than half of the samples of both NMP and NMP+HLSC-EV groups. High-Capacity cDNA Reverse Transcription Kit (Applied Biosystems^{TM}) was used to synthesize cDNA from 400 ng/µl of RNA. Then, a Real-Time PCR (Applied Biosystems^{TM}) was performed on triplicate cDNA samples according to the chemistry of Power SYBR® Green PCR Master Mix (Applied Biosystems^{TM}), using the following primers of hypoxia-induced markers:[27]

a) hypoxia-inducible factor 1-alpha (HIF-1α), forward 5'-TGTGTGTGAATTATGTTGTAAGTGGTATT-3', reverse 5'-GTGAACAGCTGG GTCATTTTCAT-3';

b) transforming growth factor-beta 1 (TGF-β1), forward 5'-TTGCCCTCTACACCAACACAA-3', reverse 5'- GGCTTGCGACCCACGTAGTA-3'.

The primer of the house-keeping gene actin β was forward 5'-ACCGTGAAA AGATGACCCAGAT-3', reverse 5'-CACAGCCTGGATGGCTACGT-3'. Comparative ΔΔCt method was used to calculate the expression levels of the genes of interest normalized to the house-keeping gene expression. One liver explant from a healthy rat (sham) was used as reference sample.

4.7 Statistical analysis

Data are expressed as mean ± standard error of the mean (SEM). Student's t-test or analysis of variance with Sidak's multi-comparison test were used where appropriate (GraphPad Prism, version 6.00, USA). A p value <0.05 was considered as statistically significant.

4.8 Results

After standardization, surgical procedures showed low variability between groups. Pre-perfusion parameters in the NMP group (n=10) were similar to those in the NMP+HLSC-EV group (n=9), regarding liver weight, tissue temperature, warm ischemia and total ischemia times. All organs were able to self-regulate pH, pO_2 and pCO_2 during the four-hour perfusion, maintaining stable flow rates and venous resistances (Table 1).

	NMP (n=10) Mean (SEM)	NMP+HLSC-EV (n=9) Mean (SEM)	p value
Liver weight [g]	10.35 (0.41)	10.16 (0.22)	0.69
Pre-perfusion temperature [°C]	13.80 (1.78)	9.89 (0.89)	0.08
Pre-perfusion ischemia time [min]			
- Warm ischemia	3.10 (0.35)	3.56 (0.24)	0.31
- Total ischemia	29.30 (1.51)	34.78 (2.39)	0.06
Flow [ml/min/g liver]			
- t = 60 min	1.23 (0.06)	1.14 (0.06)	0.33
- t = 120 min	1.30 (0.05)	1.24 (0.07)	0.49
- t = 180 min	1.30 (0.04)	1.23 (0.07)	0.41
- t = 240 min	1.19 (0.07)	1.21 (0.07)	0.80
Venous resistance [mmHg/(ml/min/g liver)]			
- t = 60 min	7.22 (0.45)	8.14 (0.47)	0.18
- t = 120 min	6.84 (0.38)	7.53 (0.47)	0.27
- t = 180 min	6.69 (0.25)	7.52 (0.43)	0.11
- t = 240 min	7.65 (0.59)	7.65 (0.45)	0.99
pH (Inflow)			
- t = 60 min	7.52 (0.09)	7.41 (0.03)	0.35
- t = 120 min	7.53 (0.09)	7.44 (0.02)	0.42
- t = 180 min	7.43 (0.06)	7.48 (0.05)	0.51
- t = 240 min	7.37 (0.08)	7.44 (0.08)	0.61
pH (Outflow)			
- t = 60 min	7.43 (0.08)	7.39 (0.06)	0.70
- t = 120 min	7.41 (0.09)	7.39 (0.03)	0.84
- t = 180 min	7.33 (0.06)	7.42 (0.04)	0.24
- t = 240 min	7.26 (0.08)	7.37 (0.05)	0.30

pO_2 (Inflow) [mmHg]			
- t = 60 min	273 (122)	240 (102)	0.84
- t = 120 min	343 (108)	273 (105)	0.66
- t = 180 min	241 (71)	290 (106)	0.75
- t = 240 min	230 (61)	239 (81)	0.93
pO_2 (Outflow) [mmHg]			
- t = 60 min	26.38 (3.67)	29.93 (3.99)	0.57
- t = 120 min	33.05 (5.06)	42.87 (7.15)	0.37
- t = 180 min	33.18 (4.78)	42.07 (6.51)	0.37
- t = 240 min	25.28 (7.40)	35.69 (4.16)	0.21
pCO_2 (Inflow) [mmHg]			
- t = 60 min	39.98 (7.67)	36.83 (4.32)	0.71
- t = 120 min	31.30 (5.34)	29.13 (3.01)	0.71
- t = 180 min	37.53 (4.86)	29.20 (1.13)	0.10
- t = 240 min	34.03 (4.40)	27.35 (3.78)	0.29
pCO_2 (Outflow) [mmHg]			
- t = 60 min	49.43 (9.12)	44.63 (4.24)	0.60
- t = 120 min	38.98 (7.96)	36.10 (2.63)	0.68
- t = 180 min	46.03 (8.46)	34.83 (1.78)	0.11
- t = 240 min	47.60 (7.17)	34.88 (3.39)	0.11

Table 1. Procedure's parameters

Immunofluorescence analysis (Figure 4) revealed the presence of DIL-stained HLSC-EV in treated livers by the end of the experiment (Figure 4C). The co-localization of HLSC-EV with the hepatocyte marker cytochrome P450-4A demonstrated their internalization within hepatocytes (Figure 4D). Histological analysis evidenced overt damage in the NMP livers, characterized by areas of necrosis and apoptosis, which were reduced in the NMP+HLSC-EV livers (Figure 4E, 4G). Tissue injury quantification by the Suzuki score (Figure 4F) showed a

significant decrease in the NMP+HLSC-EV livers (3.9±0.4) compared with the NMP ones (5.7±0.6) (p=0.030). In particular, livers treated with HLSC-EV displayed a reduced extension of necrotic areas, which never exceeded the mild degree (Figure 5). Also apoptosis was found to be significantly reduced in the NMP+HLSC-EV group (apoptosis index: 0.06±0.01 vs. 0.14±0.03, p=0.049) (Figure 4H).

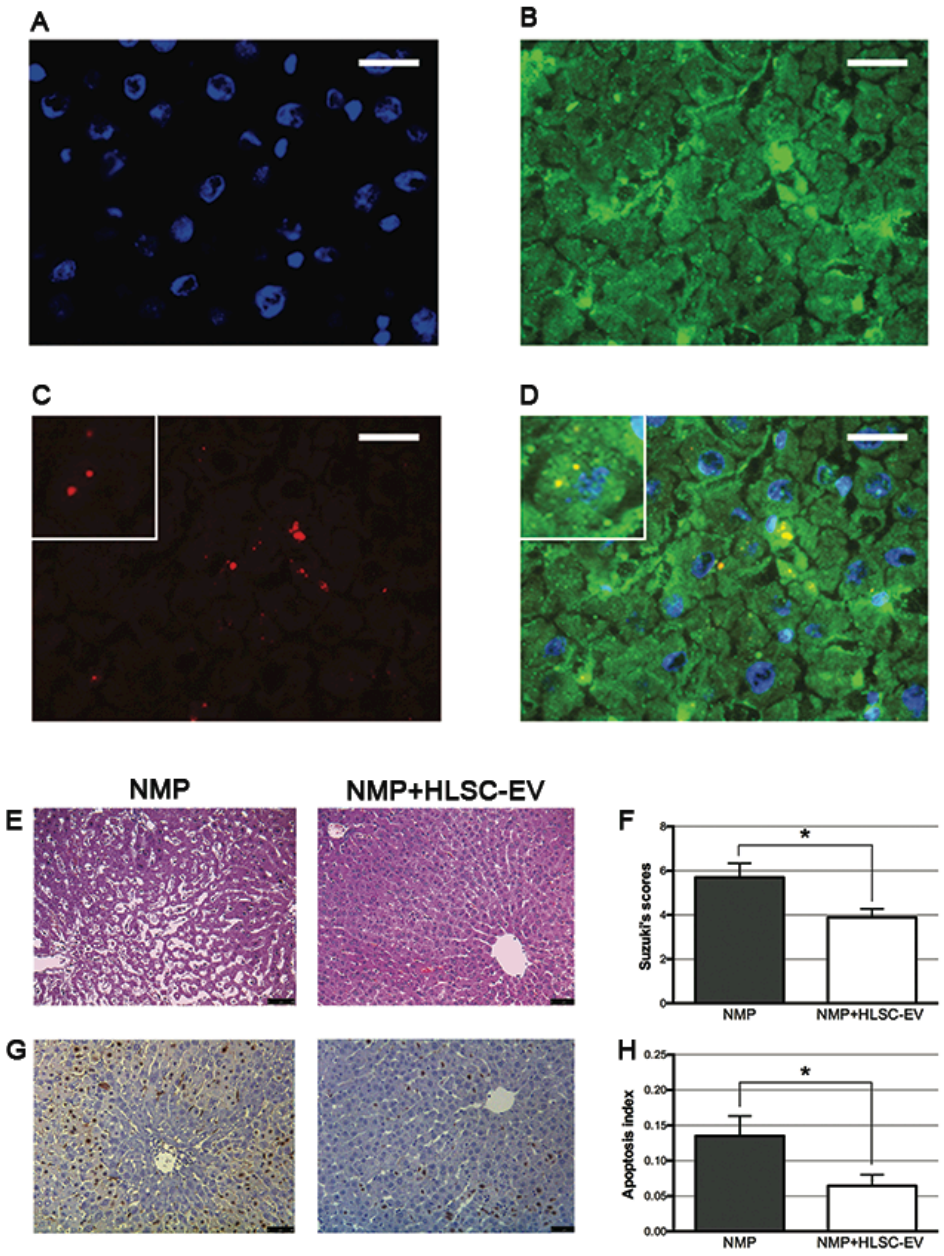

Figure 4. Immunofluorescence analysis.

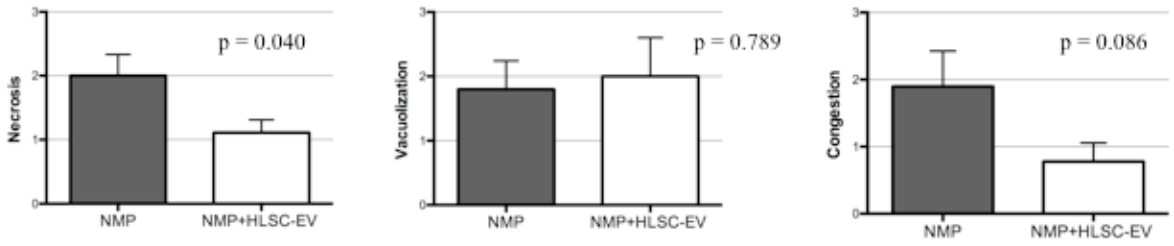

Figure 5. Suzuki Score's parameters for tissue injury.

During perfusion, biochemical analyses showed a significant gradual increase in AST, ALT and LDH levels in both NMP and NMP+HLSC-EV perfusate samples. AST, ALT and LDH reached much higher values at 4 hours than at 1 hour in each group ($p<0.0001$) (Figure 6). When compared to controls, livers treated with HLSC-EV released significantly less AST and LDH at 3 hours (AST: 92±14 vs. 47±7 U/L/g, $p=0.018$; LDH: 619±104 vs. 340±47 U/L/g, $p=0.032$) (Figure 6A, 6B) and less AST at 4 hours (134±20 vs. 80±14 U/L/g, $p=0.003$) (Figure 6A), whereas no differences were observed for ALT (Figure 6C).

Small amounts of bile were consistently produced during the *ex vivo* perfusion without differences between groups (Figure 6D).

The quantitative RT-PCR analysis showed that:

a) RNA expression of HIF-1α and TGF-β1 was increased in the NMP group, if compared to the sham reference sample (Figure 7A, 7B);

b) HLSC-EV treatment significantly reduced both HIF-1α and TGF-β1 RNA expression levels when compared to the NMP group ($p<0.0001$ and $p=0.014$, respectively) (Figure 7A, 7B).

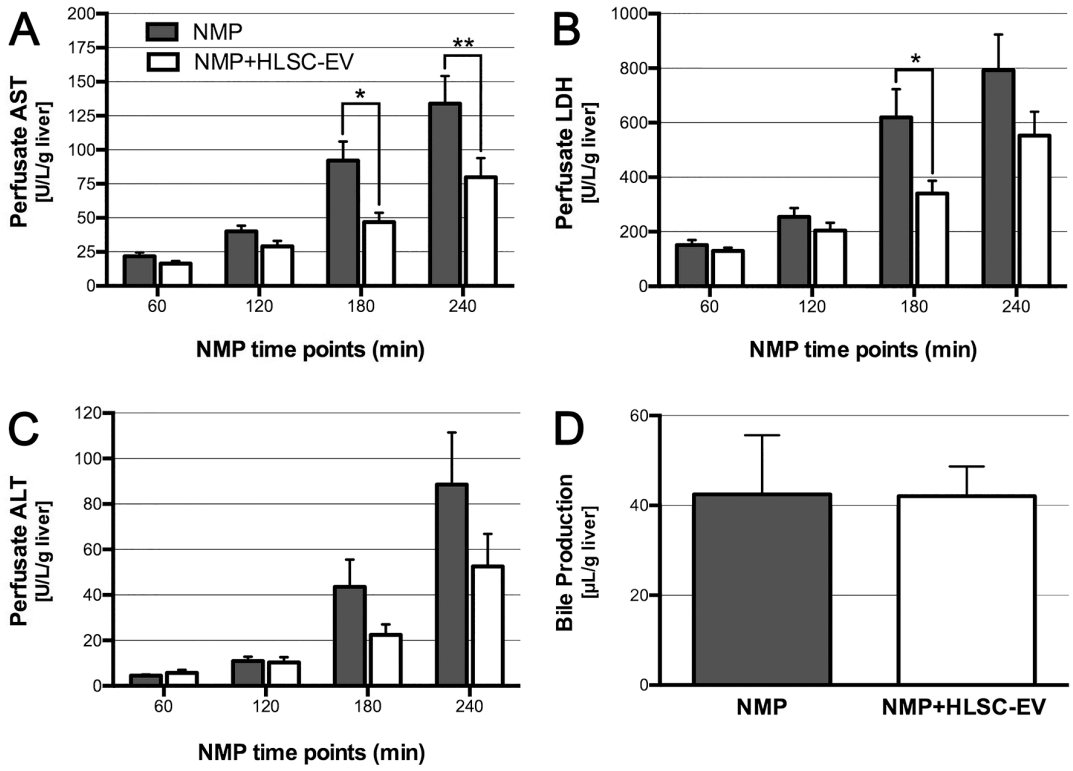

Figure 6. Biochemical analyses on perfusate and bile production.

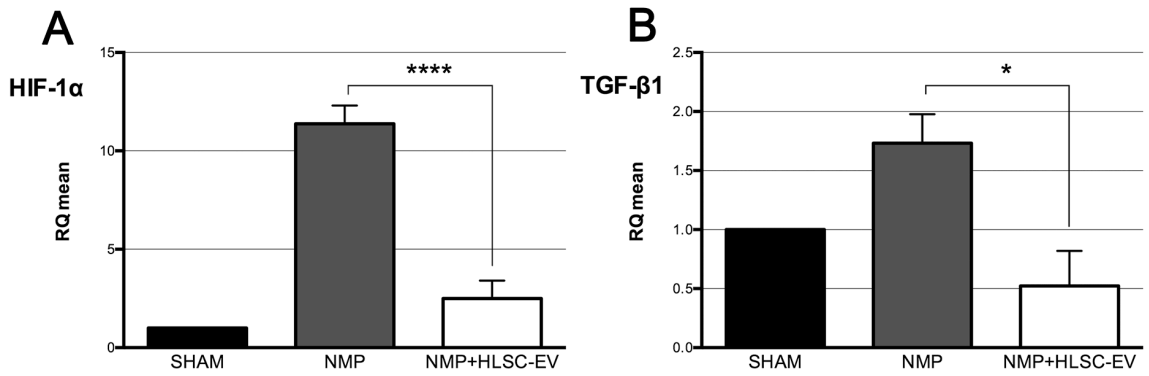

Figure 7. Quantitative RT-PCR analysis of HIF-1α and TGF-β1.

4.9 Discussion

Normothermic machine perfusion is quickly gaining recognition as a liver preservation modality capable to improve the outcomes of extended criteria grafts[16,17,18,19,20,21]. Thanks to physiological temperature and active hepatic metabolism, NMP allows to pharmacologically treat the livers[23] with the intent to ameliorate their quality prior to implantation.

HLSC are liver-resident stem-like cells, partially committed to the hepatic lineage, which carry regenerative and hepatoprotective properties[2,3]. We already demonstrated that EV derived from HLSC and mesenchymal stem cells are able to mimic most of the cell effects (including apoptosis inhibition and mitogenic activity) by transferring proteins, mRNAs and micro-RNAs[8,9,10]. Possible mechanisms involved in EV effects on injured tissue include up-regulation of anti-apoptotic genes (Bcl-xL, Bcl2, and BIRC8) and down-regulation of proapoptotic genes (Casp1, Casp8, and LTA).[5,6,10] Therefore HLSC-EV may represent a treatment option for liver diseases, avoiding stem cells transplantation.

Combining these two innovative approaches, in an *ex vivo* model of hypoxia-induced liver damage we found that HLSC-EV can be rapidly uptaken by the hepatocytes and can reduce hepatic injury, thus providing the rationale for a pharmacological intervention with HLSC-EV during NMP.

For our purpose, we set up a simplified circuit for small organs. Because of the large body of literature on isolated rat liver perfusion,[20,28,29,30] rat was chosen as the experimental animal. The morphological aspect of livers after four hours of NMP (alone or with HLSC-EV treatment) together with the maintained bile production evidenced that the experimental conditions allowed both survival and function of organs. Nonetheless, the pre-perfusion ischemic period (about 30 minutes) followed by a NMP with low hematocrit in the perfusate induced a limited but progressive hypoxic injury. This injury was proven by both the

increasing levels of cytolysis enzymes in the perfusate during perfusion and the necrotic and apoptotic areas which could be noted at the end of the experiments.

Fluorescent microscopy confirmed the ability of the rat liver to uptake HLSC-EV[8] and revealed the presence of HLSC-EV within hepatocytes at four hours. This uptake is more rapid than that observed with EV derived from mesenchymal stem cells, which were found within the injured tissue after at least five hours from their intravenous *in vivo* inoculation[11]. We hypothesize that the *ex vivo* isolated liver perfusion allows a faster and organ-specific distribution. To avoid modifications of hemodynamic parameters, we did not collect biopsy samples during perfusion; therefore, additional experiments are necessary to explore the precise timing of start of EV uptake within the liver during NMP.

In both groups, cytolysis enzyme levels gradually increased to reach a peak at the fourth hour. This trend is more likely to be ascribed to the insufficient oxygen delivery than to an *ex vivo* ischemia/reperfusion phenomenon. During this injury, in the NMP+HLSC-EV group AST and LDH were found to be lower at different time points, suggesting a protective effect of HLSC-EV against hypoxia.

The better histological integrity of the hepatic parenchyma in livers treated with HLSC-EV confirmed these findings. Moreover, HLSC-EV administered in NMP were able to reduce apoptosis by about 50%.

Finally, the RNA over-expression of hypoxia-induced markers was significantly reduced by HLSC-EV treatment. In a study on livers perfused at 37°C with an oxygen carrier deficiency, HIF-1α gene and protein expression levels were increased[30]. In our setting, EV treatment significantly limited the HIF-1α dependent response to hypoxia, replicating the evidence reported in a rat model of acute kidney injury[31]. Furthermore, a cross-talk between HIF-1 and TGF-β1, a multifunctional cytokine involved in many cellular pathways (including inflammation, apoptosis and fibrosis), was recently described in hypoxic hepatocytes[27].

All these data strongly suggest a role of HLSC-EV against hypoxic injury. Studies focusing on the characterization of HLSC-EV content are needed to clarify their mechanisms of protection.

We acknowledge that our study did not include transplantation of the livers after hypoxic NMP, yet they were overtly damaged and unsuitable for LT. We aimed indeed to investigate whether HLSC-EV could reduce hypoxic injury, a necessary proof-of-concept before proceeding to other experiments on organ preservation/reconditioning in normoxic conditions.

In conclusion, this study demonstrates that the NMP system can deliver stem cells-derived products to an *ex vivo* perfused liver, and suggests that NMP+HLSC-EV could represent an innovative approach to recondition organs before transplant. Further investigations on NMP models using HLSC-EV in other experimental conditions, including transplantation, are warranted.

5. SECOND PROJECT:

"Treatment of hepatic Ischemia Reperfusion Injury with HLSC-EV: experimental model development in the mouse"

Ischemia Reperfusion Injury (IRI) is a major issue in the clinical setting of liver transplantation and hepatic resective surgery.

While clearly unavoidable for liver transplantation, warm ischemia and reperfusion are frequently induced during hepatic resection to reduce intra-operative bleeding, by temporary clamping of the hepatic pedicle (Pringle maneuver)[32]. This may favor the onset of post-hepatectomy liver failure, which is nowadays recognized as the most dreadful complication after hepatic resection and the most frequent cause of postoperative death[33,34].

Clearly, there is a widespread interest regarding possible means to reduce this event.

The aim of this study was to investigate the effects of systemic administration of HLSC-EV on tissue injury after partial clamping of the hepatic hilum (70%) in an *in-vivo* model of IRI, that was set up in mice.

5.1 Animals

Animal studies were approved by the Ethic Committee of Istituto Superiore di Sanità (N. 62/2016-PR) and conducted in accordance with the National Institute of Health Guide for the Care and Use of Laboratory Animals. Male C57BL/6 mice, aged 10-14 weeks (20-30 g weight) obtained from Molecular Biotechnology Center (MBC) animal facility (Turin, Italy) were maintained on standard conditions and provided with food and water *ad libitum*.

In respect of the maximum number of animals indicated by ministerial directives (40 mice), preliminary analysis were performed on a total of 35 animals organized as follows:

- 3 Sham, 6 IRI and 5 IRI + HLSC-EV sacrificed after 6h
- 4 Sham, 8 IRI and 9 IRI + HLSC-EV sacrificed after 24h

Where Sham = sham operated animals; IRI = animals subjected to IRI and treated with placebo (phosphate-buffered saline); IRI + HLSC-EV = animals subjected to IRI and treated with HLSC-EV (Table 2).

	Sham	**IRI**	**IRI+HLSC-EV**
Sacrificie at 6h	3	6	5
Sacrificie at 24h	4	8	9

Table 2. Animals for preliminary analysis.

5.2 Surgical Procedure

We choose to set up un IRI's model by selective clamping of the hepatic pedicle, because it represents an experimental standard widely considered in literature[35,36,37].

Animals were anesthetized trough an intramuscolar injection of Zolazepam (0.2 mg/Kg) and Xilazyne (16 mg/Kg).

After disinfection of the skin surface, a median laparotomy of about 4 cm was performed to expose the abdominal viscera. With the use of a stereoscopic microscope (Figure 8) the liver was exposed and isolated.

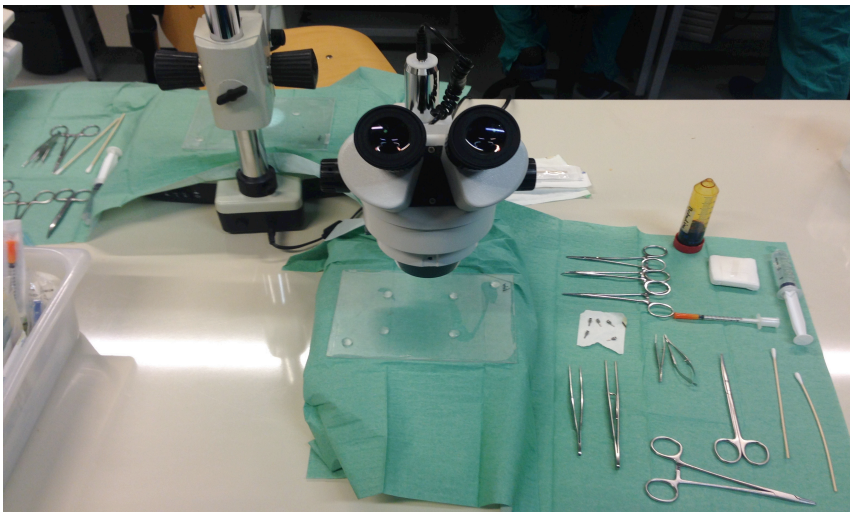

Figure 8. Surgical working base.

After the organ mobilization, ischemia-reperfusion injury was induced by temporary (90 minutes long) selective clamping of the hepatic portal pedicle for the median and left lateral lobes of the liver with an atraumatic clamp. This selective clamping allowed to induce a normothermic ischemic injury of about 70% of the hepatic parenchyma, avoiding a portal congestion that would cause haemodynamic instability and the consequent death of the animal (Figure 9). During ischemia time the animals were kept warm with an infrared lamp to avoid hypothermic crisis.

After 90 minutes the clamp was removed and the median laparotomy was closed with a 6/0 silk suture.

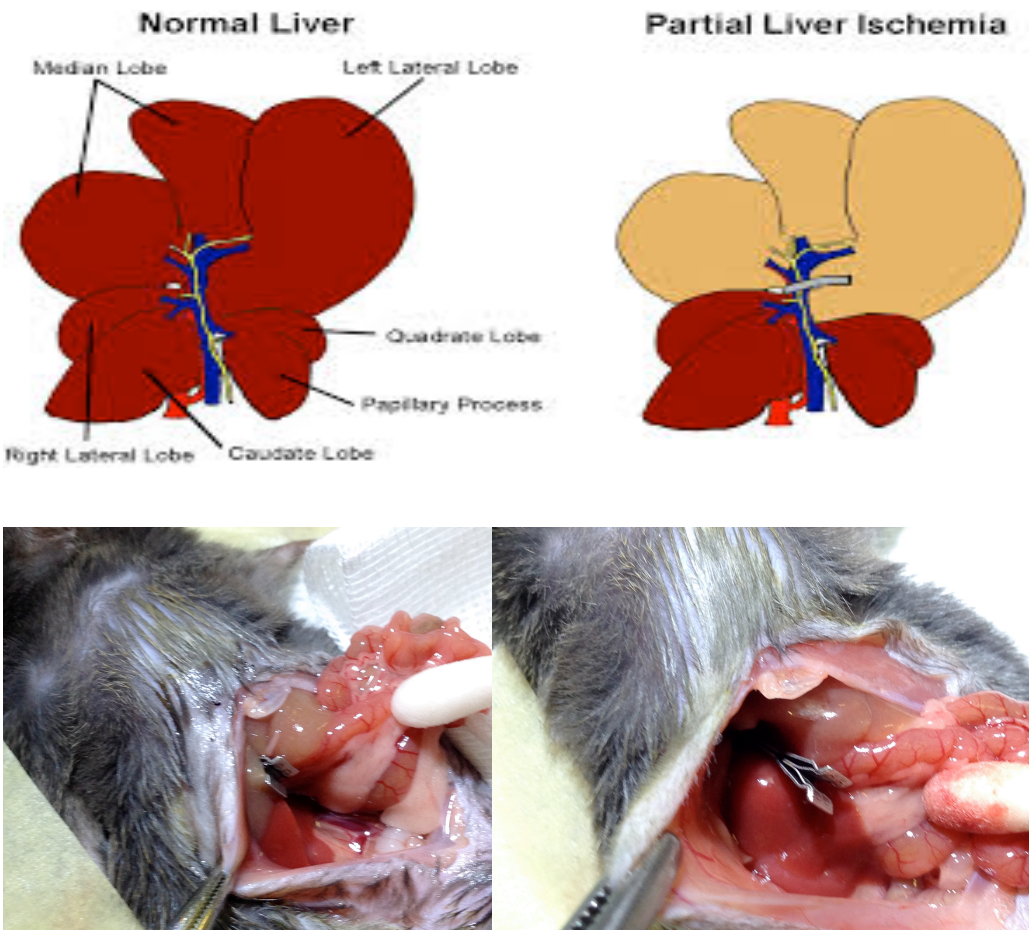

Figure 9. Surgical procedure.

At the end of the procedure, the HLSC-EV or the placebo were immediately systemically infused through the mouse's tail vein. The animal was kept under general anesthesia during the whole intervention and painkiller drugs (tramadol 2 mg/kg) were given at the end of the procedure, during awakening and anytime the animal gave signs of pain. Sham-operated animals were subjected to the same procedure, except for clamping and inoculation.

In order to evaluate the integration and biological effect of HLSC-EV, the animals' sacrifices were programmed at 6 hours and 24 hours from the end of the intervention.

At the time of sacrifice the animals were reoperated under general anesthesia (intramuscolar injection of Zolazepam 0.2 mg/Kg and Xilazyne 16 mg/Kg). The previous median laparotomy was reopened, the sternum was cut with scissors and the heart apex was punctured in order to

take 1 ml of blood for the subsequent blood tests. At the end of the procedure the animals were sacrificed by cervical dislocation and liver samples were taken from both non-ischemic lobes and lobes subjected to IRI injury.

5.3 Hystological and Immunohistochemistry analysis

Bioptic samples from both ischemic lobes and non-ischemic lobes were taken. The tissues were fixed in formalin 10% and then embedded in paraffin. For each sample, haematoxylin and eosin (H&E) stain and Proliferating Cell Nuclear Antigen-labelling (PCNA) Antibody staining were performed.

Microscopy analysis was performed using a Cell Observer SD-ApoTome laser scanning system (Carl Zeiss).

Cell proliferation was evaluated by cellular cell count. For each animal, positive and negative PCNA cells were blindly counted on 20 microscopic fields (10 from the ischemic lobe and 10 from the non-ischemic lobe) at 200× magnification, then the ratio between the number of positive cells and of total cells was calculated and considered as an indicator of cell proliferation.

5.4 Biochemical analysis

Blood samples were collected at the time of sacrifice and aspartate aminotransferase (AST), alanine aminotransferase (ALT) and lactate dehydrogenase (LDH) levels were analyzed at the Biochemistry / Clinical Laboratory - Baldi and Riberi, Molinette Hospital, Turin, Italy.

5.5 Statistical analysis

Data are expressed as mean ± standard error of the mean (SEM). Kruskal-Wallis test with Dunn correction for multiple comparisons were used where appropriate (GraphPad Prism, version 6.00, USA). A p value <0.05 was considered as statistically significant.

5.6 Results

We did not obtain the results we expected and some of them still appear to be not reliable, probably because of the small sample size. Citolysis markers (AST, ALT, LDH) levels did not show significative differences between the three populations in the 6-hours group (Figure 10A). Even though the statistical analysis does not support our first hypotesis, we strongly believe that the lack of evidence regarding the EV administration protective effect is related to the small sample size.

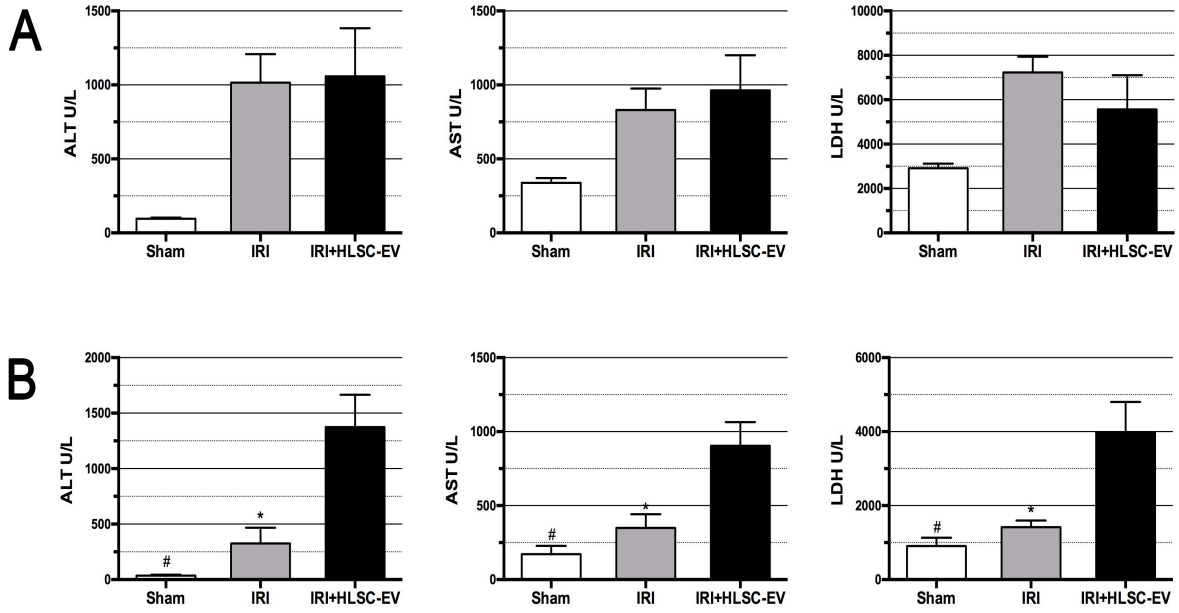

Figure 10. Biochemical analysis. **(A)** ALT, AST and LDH levels at 6 hours; **(B)** ALT, AST and LDH levels at 24 hours: ALT (*p=0.046 IRI *vs* IRI+HLSC-EV, $^{\#}$p=0.0006 sham *vs* IRI+HLSC-EV), AST (*p=0.020 IRI *vs* IRI+HLSC-EV, $^{\#}$p=0.0057 sham *vs* IRI+HLSC-EV) and LDH (*p=0.028 IRI *vs* IRI+HLSC-EV, $^{\#}$p=0.0050 sham *vs* IRI+HLSC-EV).

The analysis of the differences between populations in the 24 hours group demonstrated worst results when EV were administered (Figure 10B).

This finding is quite unexpected since no published paper reported similar observations before; the citolysis marker levels in the IRI group were significantly lower than expected and lower than standard post IRI levels; furthermore they showed no differences from the levels observed in the Sham group. Since a direct EV citolytic effect is extremely unlikely we believe that this finding is related to heterogeneity in the surgical procedures, most probably to uncomplete clamping due to the small size of the specimen.

On the other hand, the results concerning the HLSC-EV effects on cell proliferation appear to be more promising. We analized liver samples obtained at the time of sacrifice using PCNA Antibody staining. Figure 11 shows the results regarding the 24 hours group.

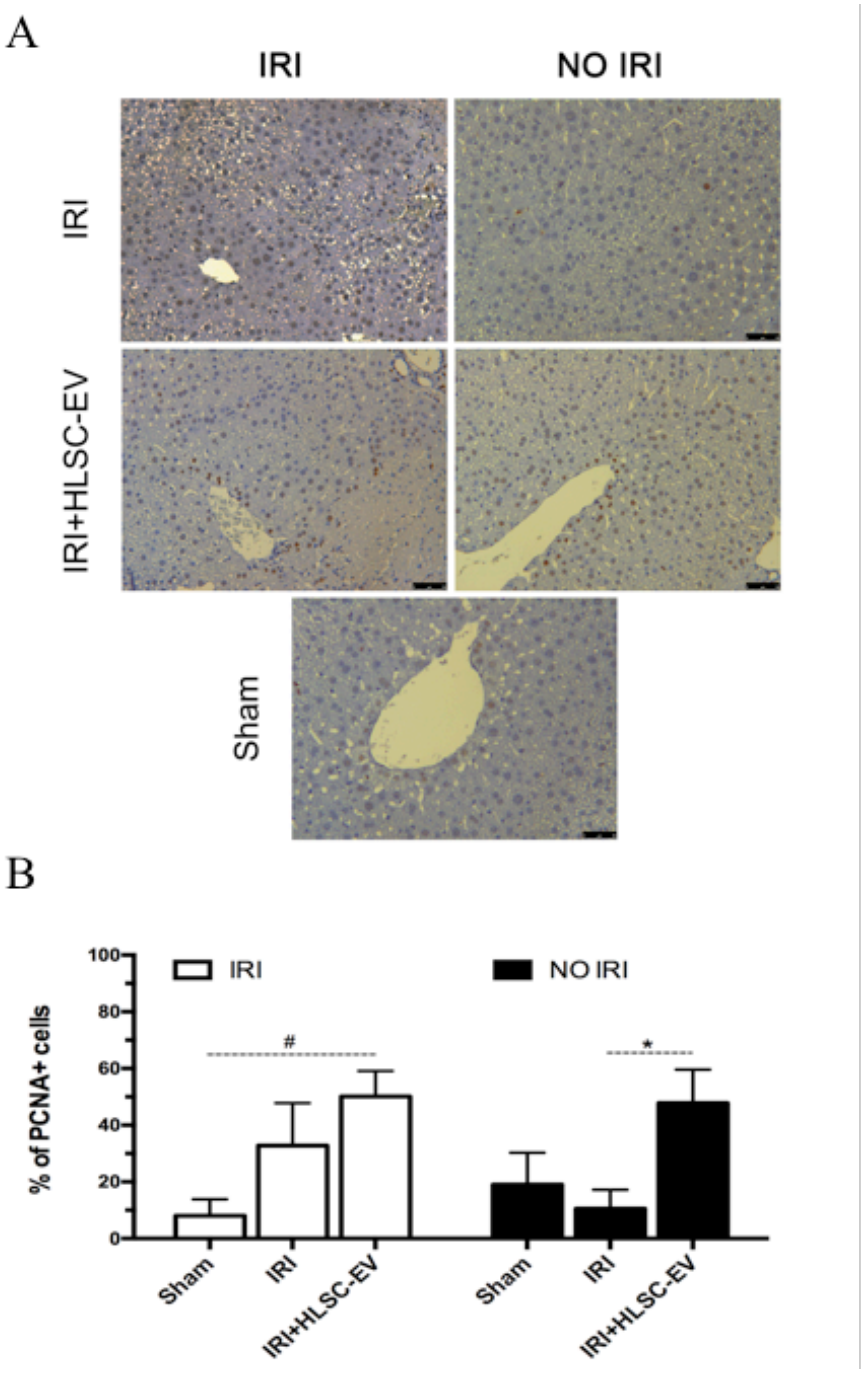

Figure 11. Immunohistochemical analysis. **(A)** PCNA staining, 200x magnification: PCNA+ cells are brown; **(B)** Percentage of PCNA+ cells on 10 microscopic fields (IRI = ischemic lobe; NO-IRI = non ischemic lobe).

#p=0.024 IRI+HLSC-EV *vs* sham; *p=0.044 IRI+HLSC-EV *vs* IRI.

Analysis were performed first on the liver parenchima where IRI was induced by vascular clamping (70% of liver parenchyma). HLSC-EV administration was associated with an increased PCNA-positive cell rate compared to the other groups; there was a significant difference between the IRI+HLSC-EV and the sham group ($p = 0.024$) and a trend of significativity when IRI and IRI+HLSC-EV groups were compared ($p = 0.12$). Again, we believe this lack of significance to be related to the small sample size.

The cell proliferation rate was also found to be significantly higher ($p = 0.044$) in the HLSC-EV group compared to the IRI group when analysis were performend on NO-IRI induced liver parenchima (30%); this observation confirms previous literarure data regarding the EV regenerative effect on healthy tissues[8]. No difference was found between the HSLC-EV and the sham group; again, this could be due to the small sample size or to the presence of an outlier in the sham group.

5.7 Discussion

Our preliminary results led us to believe that we need to make some rearrangements to our work, particularly concerning the timing of sacrifice. Recently published papers report that the regenerative effect of EV on the liver occurs early after administration; Nong et al.[38] analysed post-IRI cells replication rate after administration of EV derived from stromal mesenchimal cells and observed relevant anti-apoptotic and anti-oxidative effects at 1, 3 and 6 hours after the clamping induced vascular damage. Our previous work concerning the normothermic ex-vivo liver perfusion model also showed an HLSC-EV protective effect after

3-4 hours from the treatment, pointing out an early interaction between EV and damaged liver cells.

The heterogeneous effectiveness of vascular clamping and of EV administration, mostly related to the small size of the mice, requires adjustments in the surgical procedures as well; in particular we plan to use an easier way of EV administration through the inferior vena cava instead of the tail vein [38]. Furthermore, Haga et al.[39] have recently obtained interesting results using an higher EV dosage; we believe that an increase in EV blood concentration could lead to better results.

Given all the limitations that were mentioned above, we asked the ISS for the authorisation to continue our research and we recently obtained it.

We strongly believe that these adjustments will allow us to demonstrate the effective interaction between products derived from human liver stem cells and murine hepatocytes in the presence of ischemia / reperfusion injury and to demonstrate the biological effects on morphology and liver function.

6. REFERENCES

1 Farmer DG, Amersi F, Kupiec-Weglinski JW, Busuttil, RW. Current status of ischemia and reperfusion injury in the liver. Transplant Rev 2000;14:106.

2 Herrera MB, Bruno S, Buttiglieri S, et al. Isolation and Characterization of a Stem Cell Population from Adult Human Liver. *Stem Cells*. 2006;24:2840-2850.

3 Herrera MB, Fonsato V, Bruno S, et al. Human liver stem cells improve liver injury in a model of fulminant liver failure. *Hepatology*. 2013;57:311-319.

4 Navarro-Tableros V, Herrera MB, Figliolini F, Romagnoli R, Tetta C, Camussi G. Recellularization of Rat Liver Scaffolds by Human Liver Stem Cells. *Tissue Eng Part A*. 2015;21:1929-1939.

5 Camussi G, Deregibus MC, Cantaluppi V. Role of stem-cell-derived microvesicles in the paracrine action of stem cells. *Biochem Soc Trans*. 2013;41:283-287.

6 Quesenberry PJ, Aliotta J, Deregibus MC, Camussi G. Role of extracellular RNA-carrying vesicles in cell differentiation and reprogramming. *Stem Cell Res Ther*. 2015;6:153.

7 Biancone L, Bruno S, Deregibus MC, Tetta C, Camussi G. Therapeutic potential of mesenchymal stem cell-derived microvesicles. *Nephrol Dial Transplant*. 2012;27:3037-3042.

8 Herrera MB, Fonsato V, Gatti S, et al. Human liver stem cell-derived microvesicles accelerate hepatic regeneration in hepatectomized rats. *J Cell Mol Med*. 2010;14:1605-1618.

9 Bruno S, Grange C, Collino F, et al. Microvesicles derived from mesenchymal stem cells enhance survival in a lethal model of acute kidney injury. *PLoS One*. 2012;7:e33115.

10 Herrera MB, Bruno S, Grange C, et al. Human liver stem cells and derived extracellular vesicles improve recovery in a murine model of acute kidney injury. *Stem Cell Res Ther*. 2014;5:124.

11 Grange C, Tapparo M, Bruno S, et al. Biodistribution of mesenchymal stem cell-derived extracellular vesicles in a model of acute kidney injury monitored by optical imaging. *Int J Mol Med*. 2014;33:1055-1063.

12 Gilbo N, Catalano G, Salizzoni M, Romagnoli R. Liver graft preconditioning, preservation and reconditioning. *Dig Liver Dis*. 2016;48:1265-1274.

13 O'Callaghan JM, Morgan RD, Knight SR, Morris PJ. The effect of preservation solutions for storage of liver allografts on transplant outcomes: a systematic review and meta-analysis. *Ann Surg*. 2014;260:46-55.

14 Briceño J, Marchal T, Padillo J, Solórzano G, Pera C. Influence of marginal donors on liver preservation injury. *Transplantation*. 2002;74:522-526.

15 Ravikumar R, Leuvenink H, Friend PJ. Normothermic liver preservation: a new paradigm? *Transpl Int*. 2015;28:690-699.

16 Brockmann J, Reddy S, Coussios C, et al. Normothermic perfusion: a new paradigm for organ preservation. *Ann Surg*. 2009;250:1-6.

17 Jamieson RW, Zilvetti M, Roy D, et al. Hepatic steatosis and normothermic perfusion-preliminary experiments in a porcine model. *Transplantation*. 2011;92:289-295.

18 Butler AJ, Rees MA, Wight DGD, et al. Successful extracorporeal porcine liver perfusion for 72 hr. *Transplantation*. 2002;73:1212-1218.

19 Liu S, Pang Q, Zhang J, Zhai M, Liu S, Liu C. Machine perfusion versus cold storage of livers: a meta-analysis. *Front Med*. 2016;10:451-464.

20 Tolboom H, Pouw RE, Izamis M-L, et al. Recovery of warm ischemic rat liver grafts by normothermic extracorporeal perfusion. *Transplantation*. 2009;87:170-177.

21 Fondevila C, Hessheimer AJ, Maathuis M-HJ, et al. Superior Preservation of DCD Livers With Continuous Normothermic Perfusion. *Ann Surg*. 2011;254:1000-1007.

22 Ravikumar R, Jassem W, Mergental H, et al. Liver Transplantation After Ex Vivo Normothermic Machine Preservation: A Phase 1 (First-in-Man) Clinical Trial. *Am J Transplant*. 2016;16:1779-1787.

23 Goldaracena N, Spetzler VN, Echeverri J, et al. Inducing Hepatitis C Virus Resistance After Pig Liver Transplantation - A Proof of Concept of Liver Graft Modification Using Warm Ex Vivo Perfusion. *Am J Transplant*. 2017;17:970-978.

24 Gravante G, Ong SL, Metcalfe MS, et al. Effects of hypoxia due to isovolemic hemodilution on an ex vivo normothermic perfused liver model. *J Surg Res*. 2010;160:73-80.

25 Suzuki S, Toledo-Pereyra LH, Rodriguez FJ, Cejalvo D. Neutrophil infiltration as an important factor in liver ischemia and reperfusion injury. Modulating effects of FK506 and cyclosporine. *Transplantation*. 1993;55:1265-1272.

26 Fonsato V, Collino F, Herrera MB, et al. Human liver stem cell-derived microvesicles inhibit hepatoma growth in SCID mice by delivering antitumor microRNAs. *Stem Cells*. 2012;30:1985-1998.

27 Roth KJ, Copple BL. Role of Hypoxia-Inducible Factors in the development of liver fibrosis. *Cell Mol Gastroenterol Hepatol*. 2015;1:589-597.

28 Tolboom H, Pouw R, Uygun K, et al. A model for normothermic preservation of the rat liver. *Tissue Eng*. 2007;13:2143-2151.

29 Schlegel A, Kron P, Graf R, Dutkowski P, Clavien P-A. Warm vs. cold perfusion techniques to rescue rodent liver grafts. *J Hepatol*. 2014;61:1267-1275.

30 Ferrigno A, Di Pasqua LG, Bianchi A, Richelmi P, Vairetti M. Metabolic shift in liver: correlation between perfusion temperature and hypoxia inducible factor-1α. *World J Gastroenterol*. 2015;21:1108-1116.

31 Zou X, Gu D, Xing X, et al. Human mesenchymal stromal cell-derived extracellular vesicles alleviate renal ischemic reperfusion injury and enhance angiogenesis in rats. *Am J Transl Res*. 2016;8:4289-4

32 Ferrero A, Russolillo N, Vigano L, Lo Tesoriere R, Muratore A, Capussotti L. Does Pringle maneuver affect survival in patients with colorectal liver metastases? *World journal of surgery.* 2010;34(10):2418-.-2425.

33 Bolton JS, Fuhrman GM. Survival after resection of multiple bilobar hepatica metastases from colorectal carcinoma. *Annals of surgery*. May 2000;231(5):743-751

34 Simmonds PC, Primrose JN, Colquitt JL, Garden OJ, Poston GJ, Rees M. Surgical resection of hepatic metastases from colorectal cancer: a systematic review of published studies. *British journal of cancer*. 2006;94(7):982-999

35 Zwacka R.M., Zhang Y., Halldorson J., Schlossberg H., Dudus L., Engel- hardt J.F. CD4(þ) T-lymphocytes mediate ischemia/reperfusion-induced inflammatory responses in mouse liver. *J Clin Invest*, 1997;100(2):279-89

36 Shen X.D., Ke B., Zhai Y., Gao F., Anselmo D., Lassman C.R., et al. Stat4 and Stat6 signaling in hepatic ischemia/reperfusion injury in mice: HO-1 dependence of Stat4 disruption-mediated cytoprotection. *Hepatology*, 2003;37(2):296-303.

37 Uchida Y., Ke B., Freitas M.C., Ji H., Zhao D., Benjamin E.R., et al. The emerging role of T cell immunoglobulin mucin-1 in the mechanism of liver ischemia and reperfusion injury in the mouse. *Hepatology*, 2010;51(4):1363-72.

38 Nong K., Wang W., Niu X., Hu B., Ma C., Bai Y., Wu B., Wang Y., Ai K. Hepatoprotective effect of exosomes from human-induced pluripotent stem cell–derived mesenchymal stromal cells against hepatic ischemia-reperfusion injury in rats. *Cytotherapy*, 2016;18(12):1548-1559.

39 Haga H., Yan I.K., Takahashi K., Matsuda A., Patel T. Extracellular Vesicles from Bone Marrow-Derived Mesenchymal Stem Cells Improve Survival from Lethal Hepatic Failure in Mice. *Stem Cells Transl Med*, 2017;6(4):1262-1272.